Iranian Journal of Basic Medical Sciences
ijbms.mums.ac.ir

The role of H3K18la in regulating CDKN1B-mediated autophagy in neuropathic pain

Xiao-Jing Ou [1, 2#], Feng-Ting Zhu [1, 2#], Man-Yan Zhang [1, 2], Lang Li [2], Wei-Cheng Zhao [1, 2], Xian-Jie Wen [1, 2*]

[1] Foshan Second People's Hospital, Affiliated Hospital of Guangdong Pharmaceutical University, & Postgraduate Joint Training Base of Guangdong Medical University, Foshan, Guangdong 528000, China
[2] Department of Pain, Sleep and Psychotherapy, Foshan Second People's Hospital, Foshan, Guangdong 528000, China

ARTICLE INFO

Article type:
Original

Article history:
Received: Feb 14, 2026
Accepted: Jun 22, 2026

Keywords:
Beclin-1
Histone lactylation
L-lactate
LC3
Neuroinflammation
Neuropathic pain

ABSTRACT

Objective(s): To investigate the role of histone lactylation in chronic constriction injury (CCI)-induced neuropathic pain and elucidate its mechanism.

Materials and Methods: SD rats were assigned to Normal (n=6), CCI (n=24), and CCI+oxamate (n=24) groups; the latter two were subdivided into four time points (days 1, 4, 7, 14; n=6 each). Oxamate (300 mg/kg, IP) was given on days 0, 2, 4, 6, 10, and 12 to inhibit glycolysis. Pain behaviors were assessed. Spinal lactate and histone H3 lysine 18 lactylation (H3K18la) were measured. CUT&Tag on day 14 identified CDKN1B as an H3K18la target. A separate CDKN1B siRNA group received intrathecal siRNA on days 6, 8, 10, and 12 under oxamate treatment. Spinal IL-6, TNF-α, IL-10, Beclin-1, and LC3-II/LC3-I ratio were detected.

Results: CCI elevated spinal lactate, H3K18la, and pain, with increased inflammation compared with Normal. Oxamate reduced lactate, global H3K18la, pain, and inflammation. CUT&Tag showed higher H3K18la enrichment at the CDKN1B promoter in the oxamate group, along with up-regulated CDKN1B, Beclin-1, and the LC3-II/I ratio. CDKN1B knockdown suppressed these autophagy markers and exacerbated pain and inflammation.

Conclusion: CCI causes spinal lactate accumulation and global H3K18la up-regulation, thereby exacerbating pain and inflammation. Oxamate lowers global H3K18la but specifically increases H3K18la enrichment at the CDKN1B promoter, up-regulating CDKN1B to activate autophagy and alleviate neuropathic pain.

▶ Please cite this article as:
Ou XJ, Zhu FT, Zhang MY, Li L, Zhao WCh, Wen XJ. The role of H3K18la in regulating CDKN1B-mediated autophagy in neuropathic pain. Iran J Basic Med Sci 2026; 29:

Introduction

Studies have shown that over 30% of people worldwide are affected by chronic pain, placing a significant burden on individuals and the economy (1). Epidemiological evidence indicates that chronic pain and mental health disorders share a bidirectional relationship due to shared neural mechanisms. Patients with chronic pain commonly face mental health problems such as depression, anxiety, and suicidality, which affect their quality of life (2). Because the mechanisms underlying chronic pain are not yet fully understood and clinical treatment options and their effectiveness remain limited, chronic pain continues to be a major challenge in the field of global public health.

Chronic pain is classified into three main categories: nociceptive pain, neuropathic pain, and cancer pain. Among them, the International Association for the Study of Pain (IASP) defines neuropathic pain as pain arising from a lesion or disease of the somatosensory nervous system, and its prevalence in the general population is as high as 6.9–10% (3). Symptoms commonly include hypersensitivity characterized by spontaneous pain, allodynia, and hyperalgesia. The mechanisms underlying neuropathic pain are complex and involve multiple biological processes, such as peripheral sensitization, central sensitization, neuroinflammation, alterations in ion channels, and changes in neuroplasticity (4).

Autophagy is a highly conserved adaptive response to cellular stress, widely present in eukaryotes, and serves as a tightly regulated "self-clearance" mechanism. During this process, cytoplasmic components such as misfolded proteins, damaged organelles, or endogenous pathogens are sequestered into double-membrane autophagosomes and delivered to lysosomes for degradation and recycling (5). Studies indicate that enhanced autophagic activity may facilitate the clearance of myelin debris, aid nerve repair, and reduce pain-related behaviors; moreover, autophagy may further reduce pain manifestations by inhibiting pro-inflammatory cytokine activity (6).

Epigenetic mechanisms hold great potential in the field of pain. Recent clinical studies have indicated that the epigenetic

*Corresponding author: Xian-Jie Wen. No. 78, Weiguo Road, Chancheng District, Foshan City, Guangdong Province 528000, China. Email: xjwen166@163.com
#These authors contributed eqully to this work

regulation of transcription in nociceptive pathways through histone post-translational modifications (PTMs) is innovative. Yet, current research has largely centered on histone methylation, acetylation, phosphorylation, and ubiquitination (7-8). For instance, studies have shown that a dual-target inhibitor of bromodomain-containing protein 4 (BRD4) and histone deacetylase (HDAC) can attenuate the pro-inflammatory response of microglia, thereby relieving neuropathic pain (9). In 2019, Zhao Yingming's team first proposed in Nature that "histone lactylation can serve as a novel epigenetic modification with the function of regulating gene transcription" (10). Researchers have gradually turned their focus to the mechanisms involving lactate and histone lactylation. As research has deepened, histone lactylation has been confirmed to be widely involved in the pathophysiological processes of diverse diseases (11). Although a large number of studies have demonstrated a strong link between lactate and pain perception (12-13)—lactate can not only directly stimulate chronic pain-associated receptors and neurons, but also modulate pain through astrocyte-neuron lactate transport—the role of histone lactylation in pain, especially in neuropathic pain, remains unclear.

Based on the research status described above, this study aims to investigate the role of histone lactylation in neuropathic pain in a rat model of chronic constriction injury (CCI) of the sciatic nerve, and to preliminarily analyze the underlying mechanisms by establishing the CCI model and intraperitoneally injecting sodium oxamate to inhibit glycolysis in the spinal cord tissue of CCI rats.

Materials and Methods

Experimental animals

Male Sprague-Dawley (SD) rats (6–8 weeks old, weighing 180–200 g) were purchased from Guangdong Weitong Lihua Laboratory Animal Technology Co., Ltd., and the experimental animals were of specific pathogen-free (SPF) grade. The housing conditions included a clean and ventilated environment, a stable temperature of 22–24 °C, humidity of 50±5%, and a 12/12 hr light/dark cycle, with free access to food and water. All procedures strictly followed the guidelines for the use and care of laboratory animals issued by the International Association for the Study of Pain (IASP) and were approved by the Experimental Animal Ethics Committee of Guangdong Medical Laboratory Animal Center (ethics number C202309-38).

Animal grouping, CCI model establishment, and intrathecal injection

Seventy-two SD rats were randomly divided into the following six groups: normal control group (Normal, n=6), sham operation group (Sham, n=6), sciatic nerve ligation group (CCI, n=24), sciatic nerve ligation + sodium oxamate group (Oxamate, n=24), sciatic nerve ligation+sodium oxamate+CDKN1B siRNA group (abbreviated as CDKN1B, n=6), and sciatic nerve ligation + sodium oxamate + negative control siRNA group (abbreviated as NC, n=6). Among them, the CCI group and the Oxamate group were further divided into four subgroups according to the observation time points (postoperative days 1, 4, 7, and 14), with 6 rats in each subgroup; the CDKN1B group and the NC group were sampled on postoperative day 14 (corresponding to the day-14 subgroups of the CCI and Oxamate groups).

The CCI model was established using the method described by Bennett et al. (14). After a 12-hour preoperative fast, rats were anesthetized with 3% isoflurane inhalation and placed in the prone position. A 1.5–2 cm longitudinal skin incision was made on the lateral aspect of the mid-femur of the left hindlimb. The biceps femoris muscle was bluntly separated to expose the main trunk of the sciatic nerve, and a segment approximately 7–10 mm in length was freed. Three ligatures were tied around the nerve trunk using 4-0 silk suture, with an inter-ligature spacing of about 1 mm. The ligation strength elicited slight muscle twitching of the ipsilateral hindlimb without compromising the blood supply to the epineurium. The incision was closed in layers and disinfected with povidone-iodine. The rats were placed on a heating pad until they regained consciousness and were then given free access to water and food postoperatively.

The treatments for each group were as follows: Normal rats received no intervention; Sham rats underwent only sciatic nerve exposure without ligation; CCI rats received CCI modeling without any drug administration. In the Oxamate group, sodium oxamate (300 mg/kg, dissolved in 0.9% NaCl, S818460, Macklin) was administered intraperitoneally on the day of surgery and on postoperative days 2, 4, 6, 8, 10, and 12 (15). Sodium oxamate competitively binds to the NADH-binding site of lactate dehydrogenase (LDH), thereby inhibiting LDH activity, blocking the conversion of pyruvate to L-lactate, and effectively reducing endogenous L-lactate levels in spinal cord tissue. In this study, "glycolysis inhibition" specifically refers to this pharmacological reduction of lactate availability. In the CDKN1B group, based on the Oxamate treatment, rats received intrathecal injections of CDKN1B siRNA (1 μg/μl, 10 μl) on postoperative days 6, 8, 10, and 12 (16); the NC group received equal volumes of negative control siRNA via the same route. The timing of intrathecal injections was chosen based on our preliminary data showing that CDKN1B mRNA expression in the Oxamate group became significantly different from the CCI group starting on day 7, ensuring alignment of the intervention window with the target gene expression kinetics.

The intrathecal injection procedure was as follows: anesthesia was first induced with 3% isoflurane using a small animal anesthesia machine (MW-IA5). Subsequently, the dorsal hair over the L3 to S1 segments was shaved, the surgical area was disinfected with povidone-iodine, and a sterile surgical drape was placed. The rat was fixed in the prone position on a thermostatic operating table set to 37±0.5 °C. The left thumb and middle finger were used to hold the posterior superior iliac spines, while the right palm gently pressed on the sacrum to produce a moderate arching of the spine at the L4–L6 level; the index finger was palpated to locate the L5–L6 intervertebral space. The needle was inserted perpendicularly through the skin, and a "pop" sensation was felt when penetrating the ligamentum flavum. The appearance of cerebrospinal fluid upon aspiration, sometimes accompanied by a slight flick of the rat's tail, indicated that the needle tip had entered the subarachnoid space (17). All siRNA sequences were synthesized by Guangzhou Yige Biotechnology Co., Ltd. (IGEBio), and the gene sequences are detailed in Table 1.

Behavioral tests

The mechanical withdrawal threshold and thermal

Table 1. CDKN1B siRNA and negative control siRNA sequences used to investigate the effect of CDKN1B knockdown on neuropathic pain in rats

Name		Sequence (5'-3')
CDKN1B	Sense	GGUCAAUCAUGAAGAACUAtt
	Antisense	UAGUUCUUCAUGAUUGACCtt
NC	Sense	UUCUCCGAACGUGUCACGUtt
	Antisense	ACGUGACACGUUCGGAGAAtt

withdrawal latency of the left hindpaw were assessed before surgery and on postoperative days 1, 4, 7, and 14 using the methods described below. The testing environment was maintained at 23±1 °C, 50±5% humidity, and background noise below 40 dB. Before testing, the rats were placed in a transparent acrylic chamber (30×30×30 cm) with a stainless-steel mesh floor (3 mm aperture) and allowed to habituate for 15 min. The chamber was surrounded by black cloth to block light.

Mechanical withdrawal threshold (MWT): The 50% mechanical threshold was determined using the up-down method (18). A von Frey filament was applied perpendicularly to the same site on the plantar surface of the left hindpaw, with a duration of ≤4 sec. Rapid paw withdrawal, leg shaking, or licking was considered a positive response. Beginning at 2 g, the stimulus intensity was increased if no response was observed and decreased if a response occurred. A sequence of five responses containing at least three turning points was recorded, and the 50% threshold was calculated according to the formula. The maximum threshold was set at 15 g and the minimum at 0.008 g. The interval between stimuli was ≥30 sec, and each paw was tested no more than 7 times per day.

Thermal withdrawal latency (TWL): TWL was measured using a thermal pain stimulator (BME-410C) (19). The light from a mobile halogen-tungsten lamp was focused on the plantar surface of the left hindpaw. The timer was started automatically when the light was turned on and stopped when the rat exhibited rapid paw withdrawal, flinching, or licking, and the latency was recorded. A cut-off time of 25 s was set to prevent tissue injury. Each rat was tested three times, with an interval of at least 5 min between tests, and the mean value was used as the final thermal threshold.

Cut &Tag

Library construction and sequencing for Cut&Tag

According to the manufacturer's instructions, Cut&Tag was performed on spinal cord tissues collected on day 14 using the Novoprotein NovoNGS™ Cut&Tag High-Sensitivity Kit (Cat. No. N259-YH01-01B). At room temperature, ConA-coated magnetic beads were incubated with tissue samples from the Normal, CCI, and Oxamate groups for 10 min. After the supernatant was removed, an anti-H3K18la primary antibody (PTM-1406RM, PTM BIO) was added and incubated overnight at 4 °C. On the following day, the samples were incubated with a secondary antibody for 1 hr at room temperature with rotation to complete antibody labeling. The samples were then incubated with pA-Tn5 transposase to fragment the target chromatin regions. The fragmentation reaction was carried out at 37 °C for 1 hr, and the DNA was subsequently purified using Tagment DNA Extract Beads. The obtained DNA fragments were amplified by PCR, and the amplified products were purified with magnetic beads to construct the library. Finally, after passing quality control, the libraries were sequenced on the Illumina NovaSeq platform to obtain high-quality data for subsequent bioinformatic analysis.

Data analysis and quantification

After quality control of the raw sequencing data with FastQC (v0.12.1), the raw reads were filtered using cutadapt software (removing adapters, low-quality reads, and short reads, etc.) to obtain clean reads. The clean reads were then aligned to the rat reference genome (rn7) using Bowtie2 (v2.5.1). Based on the alignment results, the fragment size distribution, inter-sample correlation, and signal distribution characteristics across gene regions were assessed with deeptools (v3.5.1). Peak calling was performed using MACS2 (v2.2.9.1) in broad peak mode, with the effective genome size set to 2.7e9 and a broad peak significance threshold of 0.05. Using the IgG antibody sample from the same experimental batch as a negative control, the fold enrichment and false discovery rate (FDR) for each peak were calculated, and peaks with FDR<0.05 and fold enrichment ≥ 2 were retained as high-confidence H3K18la binding regions. Differential peak analysis between groups was further conducted using the DESeq2 algorithm implemented in the R package, with thresholds of ***P*<0.05** and |log2FC| ≥ 1 to identify peak regions significantly different among groups. Peak annotation and enrichment analysis were performed using ChIPseeker (v1.34.1) and clusterProfiler (v4.6.2), respectively (padj<0.05). All data processing and statistical analyses were carried out in the R (v4.4.0) and Python (v3.10) environments.

Western blot

Lumbar spinal cord enlargement tissues were collected from rats before surgery and on postoperative days 1, 4, 7, and 14, and total protein was extracted for western blot analysis. The spinal cord tissues were washed with pre-cooled PBS, homogenized, and then thoroughly lysed in RIPA lysis buffer containing protease inhibitors. After centrifugation, the supernatant was collected. Protein concentrations were determined using the BCA assay, and the loading amounts of each sample were adjusted to ensure consistency. The proteins were heat-denatured, separated by SDS-PAGE, and transferred to PVDF membranes. The membranes were blocked with TBST containing 5% non-fat dry milk for 1 hr at room temperature, followed by overnight incubation with specific primary antibodies at 4 °C. After washes with TBST, the membranes were incubated with HRP-conjugated secondary antibodies for 1 hr at room temperature, washed again, and visualized by ECL chemiluminescence. The optical densities of the bands were quantified using AlphaEaseFC software.

The primary antibodies used in this study were: rabbit monoclonal anti-H3K18la (PTM-1406RM, PTM BIO, 1:1000); rabbit monoclonal anti-H4K12la (PTM-1411RM, PTM BIO, 1:1000); rabbit anti-CDKN1B (#3686, CST, 1:2000); rabbit anti-Beclin-1 (#3495, CST, 1:1000); rabbit

anti-LC3 (#4108, CST, 1:500); and rabbit anti-β-Actin (TDY051, TianDeYue, 1:10000). The secondary antibody was HRP-conjugated goat anti-rabbit IgG (AS1245, ASPEN, 1:10000).

Lactate content measurement

L-lactate (A019-2-1, Jiancheng) and D-lactate (A019-3-1, Jiancheng) colorimetric assay kits were used to measure lactate content in the spinal cord tissue of rats, respectively.

L-lactate

Spinal cord tissue was weighed, and pre-cooled normal saline was added at a ratio of 1:9 (w/v). The tissue was homogenized in an ice bath (2500 rpm, 10 min) and centrifuged at 3000×g for 10 min at 4 °C, after which the supernatant was collected. Blank tubes (distilled water), standard tubes (3 mmol/l lactate standard), and test tubes (samples to be measured) were set up. Enzyme working solution and chromogenic agent were added sequentially, mixed well, and then the mixture was incubated in a 37 °C water bath for 10 min, after which stop solution was added. The absorbance was measured at 530 nm with distilled water as the blank. The lactate concentration of the samples was calculated based on the standard and expressed as mmol/g protein.

D-lactate

Extraction solution was added at a ratio of 1:10 (w/v), and the tissue was homogenized at 4 °C and centrifuged at 8000–12000 × g for 10 min, after which the supernatant was collected. The sample and reagents were added to the reaction system, incubated at 37 °C in the dark for 30 min, and the absorbance was measured at 450 nm. D-lactate content was calculated using a standard curve and expressed as μmol/g protein.

ELISA

Lumbar spinal cord tissues were collected from rats before surgery and on postoperative days 1, 4, 7, and 14, and the levels of the inflammatory cytokines IL-6 (ELK1158), IL-10 (ELK1144), and TNF-α (ELK1396) were measured using double-antibody sandwich ELISA kits. For every 100 mg of tissue, 900 μl of PBS lysis buffer containing protease inhibitors was added. After homogenization, the homogenate was centrifuged at 10,000×g for 5 min at 4 °C, and the supernatant was collected. The subsequent steps were performed following the manufacturer's instructions: standards or samples (100 μl/well) were added to the pre-coated microplate and incubated at 37 °C for 80 min; after the liquid was discarded, biotin-labeled antibody working solution (100 μl/well) was added and incubated at 37 °C for 50 min; after washing, streptavidin-HRP working solution was added and incubated at 37 °C for 50 min; after washing, TMB substrate was added for color development in the dark for 15 min, and the reaction was terminated by adding stop solution. The optical density (OD) was measured immediately at 450 nm using a microplate reader. The concentration of each cytokine was calculated from the standard curve, and the results were expressed as pg/mg total protein (total protein concentration was determined by the BCA assay).In this study, we measured these three cytokines using ELISA. We operationally define "inflammation suppression" as a decrease in IL-6 and TNF-α together with an increase in IL-10, and use this combined pattern as a quantitative indicator of inflammatory relief.

Table 2. Primer sequences used for real-time quantitative PCR analysis of CDKN1B

Gene name	Primer sequence (5'→3')
R-ACTIN	F:CGTTGACATCCGTAAAGACCTC
	R:TAGGAGCCAGGGCAGTAATCT
R-CDKN1B	F:GATACGAGTGGCAGGAGGTG
	R:GTCTGACGAGTCAGGCATTTG

Real-time quantitative PCR (qPCR)

Lumbar spinal cord enlargement tissues were collected from rats before surgery and on postoperative days 1, 4, 7, and 14 to detect the mRNA expression level of CDKN1B. The primer sequences are shown in Table 2.

Approximately 20 mg of tissue was taken, ground in pre-cooled TRIpure reagent, and then chloroform was added for phase separation. After centrifugation, the supernatant was collected, and RNA was precipitated with isopropanol, washed with 75% ethanol, and dissolved in RNase-Free Water. Subsequently, cDNA was synthesized using the EntiLink™ First-Strand cDNA Synthesis Kit (ELK Biotechnology, EQ003) according to the manufacturer's instructions: total RNA was mixed with primers, pre-denatured at 70 °C for 5 min, extended at 37 °C for 60 min, and inactivated at 85 °C for 5 min. Next, using the synthesized cDNA as template, amplification was performed on a QuantStudio 6 Flex real-time PCR system with the EnTurbo™ SYBR Green PCR SuperMix Kit (ELK Biotechnology, EQ001). The reaction program was as follows: pre-denaturation at 95 °C for 3 min; 40 cycles of 95 °C for 10 sec, 58 °C for 30 sec, and 72 °C for 30 s; followed by a melting curve acquisition (95 °C for 15 sec, 60 °C for 1 min, and 95 °C for 15 s) to verify specificity. β-actin was used as the internal reference, and the relative expression was calculated using the 2^−ΔΔCt method. Each sample was run in triplicate.

Statistical analysis

All statistical analyses were performed using SPSS 25.0 software. Data are expressed as mean±standard error of the mean (SEM). For repeated-measures data such as behavioral tests, two-way repeated-measures ANOVA was used, with group and time as main factors and their interaction tested. For independent observations such as biochemical assays, one-way or two-way ANOVA was applied depending on the number of groups. Following each ANOVA, Tukey's post-hoc test was performed for multiple pairwise comparisons. Before parametric testing, normality was assessed by the Shapiro–Wilk test and homogeneity of variances by Levene's test; if these assumptions were violated, non-parametric tests were applied instead. A P-value<0.05 was considered statistically significant.

Results

Expression levels of L-lactate and H3K18la in the spinal cord of CCI rats

To explore the main precursor lactate types and their level changes involved in histone lactylation in the spinal cord enlargement tissue after CCI, lactate content in the spinal cord tissue of rats was measured using colorimetric assays. The colorimetric assays showed that after sciatic nerve ligation, the expression of L-lactate increased

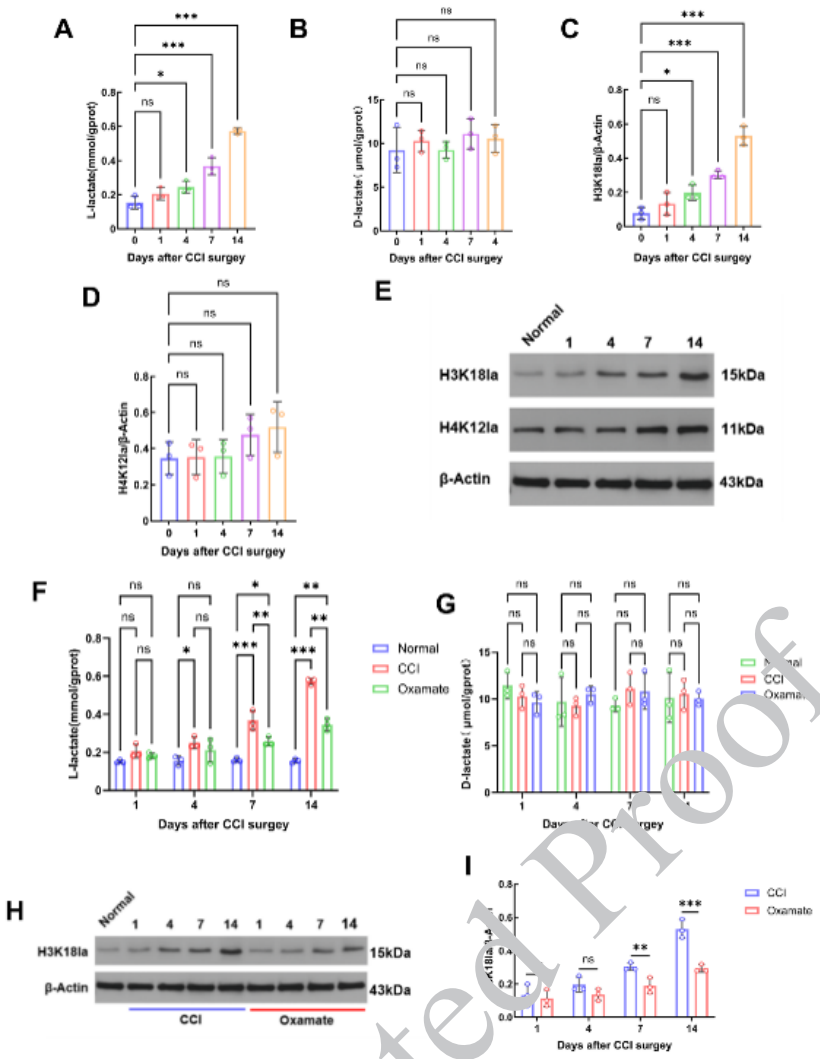

Figure 1. Effect of sodium oxamate on L-lactate levels and histone lactylation in the spinal cord of CCI rats
(A–B) Time-course changes of L-lactate (A) and D-lactate (B) content in the spinal cord before surgery and on postoperative days 1, 4, 7, and 14 in CCI rats.
(C–E) Quantification of H3K18la (C) and H4K12la (D) and representative western blot images (E) in spinal cord tissues at the corresponding time points, with β-actin as the loading control.
(F–G) Comparison of L-lactate (F) and D-lactate (G) levels among the Normal, CCI, and Oxamate groups at the indicated time points.
(H–I) Western blot analysis and quantification of H3K18la across different time points in the spinal cord of the three groups.
Data are expressed as mean±SD (n=3 rats per group). *P<0.05, **P<0.01, ***P<0.001; ns, not significant. For panels (A–E), which examined time-course changes within the CCI group, comparisons among different time points were performed using one-way ANOVA followed by Tukey's *post hoc* test. For panels (F–I), which involved comparisons across groups and time points, two-way ANOVA followed by Tukey's *post hoc* test was used to assess the effects of group, time, and their interaction.
CCI: Chronic constriction injury; H3K18la: Histone H3 lysine 18 lactylation; H4K12la: Histone H4 lysine 12 lactylation

significantly from postoperative day 4 to day 14. In contrast, D-lactate showed no statistically significant difference at any observation time point, as illustrated in Figure 1A and B, suggesting that L-lactate is more likely to be the main precursor substance involved in histone lactylation modification during this process. Previous studies have found that in a spinal cord injury (SCI) model, western blotting using different types of histone lactylation antibodies revealed increased levels of H3K18la and H4K12la (20). To explore the histone lactylation sites in the spinal cord tissue after CCI, we selected H3K18la and H4K12la antibodies for western blotting detection. The results showed that the lactylation expression level of H3K18la in the spinal cord tissue was significantly elevated from day 4 onward, whereas H4K12la showed no statistically significant difference at any observation time point, as shown in Figure 1 C–E. These results indicate that histone lactylation modification in the spinal cord tissue after sciatic nerve ligation exhibits site specificity, and its dynamic changes are temporally consistent with the rise in L-lactate levels, further supporting the potential role of L-lactate as a key precursor molecule in this pathological process.

Inhibition of glycolysis reduces lactate content and H3K18la expression in the spinal cord

Compared with the CCI group, after inhibition of glycolysis by intraperitoneal injection of the glycolysis inhibitor sodium oxamate, the level of L-lactate in the spinal cord tissue of the Oxamate group was significantly decreased from day 7 onward. Still, its content remained significantly higher than that of the control group from day 7 to day 14. Throughout the observation period, there were no statistically significant differences in D-lactate content among the control, CCI, and Oxamate groups. No statistically significant differences within each group, as shown in Figure 1 F and G. Western blot analysis further indicated that after oxamate intervention, the expression level of H3K18la in the spinal cord tissue of rats in the Oxamate group was also

Table 3. Summary of rat behavioral data

A: Thermal withdrawal latency in each experimental group					
Group	T0	T1	T2	T3	T4
Normal	18.32±1.00	18.17±0.67	18.51±1.45	18.78±1.01	18.48±0.78
Sham	18.56±0.51	17.82±0.58	18.32±0.89	17.95±0.64	18.38±0.96
NC	18.39±0.53	17.62±0.51	13.67±1.08[ab]	13.66±0.63[ab]	12.06±0.71[ab]
CCI	18.22±0.99	17.67±1.05	12.24±1.6[ac]	10.31±1.41[ac]	9.26±1.41[ac]
Oxamate	18.11±0.79	17.68±0.87	13.56±1.18[ab]	12.74±1.18[ab]	12.54±0.88[ab]
CDKN1B	18.43±0.98	17.77±1.49	14.04±0.57[ab]	11.87±1.75[ab]	9.88±0.76[ac]
B: Mechanical withdrawal threshold in each experimental group					
Group	T0	T1	T2	T3	T4
Normal	13.41±2.58	13.71±2.44	13.41±2.58	13.41±2.58	13.12±2.67
Sham	13.00±3.16	13.33±2.58	13.33±2.58	13.33±2.58	13.33±2.58
NC	13.33±2.58	13.00±3.16	9.67±0.82[ab]	8.33±1.51[ab]	6.67±1.03[ab]
CCI	13.76±2.28	13.32±2.48	7.76±2.33[ac]	5.09±2.51[ac]	3.41±2.63[ac]
Oxamate	13.41±3.08	13.76±2.28	9.96±1.99[ab]	8.45±1.63[ab]	6.50±1.86[ab]
CDKN1B	13.13±2.59	13.50±2.83	9.75±0.71[ab]	8.25±1.28[ab]	4.[illegible]±1.51[ac]

Data are presented as mean±SD, n=6. [a]P<0.05 vs Normal group; [b]P<0.05 vs CCI group; [c]P<0.05 vs Oxamate group.T0, baseline (before surgery); T1, postoperative day 1; T2, day 4; T3, day 7; T4, day 14.Statistical comparisons were performed by two-way ANOVA followed by Tukey's post hoc test. Thermal withdrawal latency is expressed in seconds (s), and mechanical withdrawal threshold is expressed in grams (g).
CCI: Chronic constriction injury; CN: Negative control; CDKN1B: Cyclin-dependent kinase inhibitor 1B

significantly decreased from day 7 compared with the CCI group, but remained higher than that of the control group, as shown in Figure 1 H and I. Notably, the change trend of L-lactate and the expression level of H3K18la exhibited temporal concordance; that is, after sciatic nerve ligation, both L-lactate content and H3K18la expression level in the spinal cord tissue of rats were significantly increased on postoperative day 4. Both were significantly decreased on postoperative day 7 following oxamate intervention. This result further supports the potential role of L-lactate as a precursor molecule for lactylation modification at the H3K18 site, suggesting that glycolysis-derived L-lactate plays an important role in regulating histone lactylation.

Effect of inhibiting lactate production on the behavior of CCI rats

Based on current research, a close link exists between lactate and pain perception (21). To verify the relationship between lactate and pain in the CCI model, the present study conducted behavioral tests, including the mechanical withdrawal threshold (MWT) and thermal withdrawal latency (TWL), on rats in each group before surgery and on postoperative days 1, 4, 7, and 14. Statistical analysis showed that compared with the Normal group, the CCI group exhibited a significant decrease in pain threshold from postoperative day 4 onward, manifesting as mechanical and thermal hyperalgesia. After oxamate intervention, the pain threshold of rats in the Oxamate group showed a certain degree of recovery from day 4, with a statistically significant difference compared with the CCI group, indicating that inhibition of glycolysis can partially alleviate CCI-induced hyperalgesia. Notably, although sodium oxamate improved the pain behavior of rats following sciatic nerve ligation, their pain threshold levels remained significantly lower than those of normal rats, suggesting that this intervention did not completely reverse the nociceptive changes induced by nerve ligation. Detailed data are presented in Table 3 and Figure 2 B-C.

Effect of glycolysis inhibition on the expression of inflammatory cytokines in the spinal cord tissue of CCI rats

To investigate whether glycolysis inhibition alleviates pain by reducing inflammation, we measured the expression of inflammatory cytokines in the spinal cord tissue of rats in the Normal, CCI, and Oxamate groups. The results showed that compared with the Normal group, the expression of the pro-inflammatory cytokines IL-6 and TNF-α in the CCI group increased significantly from day 4 onward. In contrast, the anti-inflammatory cytokine IL-10 decreased significantly. After oxamate intervention, compared with the CCI group, the levels of IL-6 and TNF-α in the Oxamate group decreased significantly from day 4 onward. At the same time, the expression level of IL-10 increased significantly, suggesting that glycolysis inhibition can restore the inflammatory balance to a certain extent. However, compared with the Normal group, the Oxamate group still exhibited an imbalance with increased pro-inflammatory cytokines IL-6 and TNF-α. It decreased the anti-inflammatory cytokine IL-10, as shown in Figure 2 F-H. The above results indicate that glycolysis inhibition may alleviate neuropathic pain in CCI rats by partially correcting the imbalance between pro-inflammatory and anti-inflammatory cytokines.

Effect of glycolysis inhibition on CDKN1B gene expression in CCI rats

Previous studies have demonstrated that histone lactylation modification contributes to the transcriptional regulation of downstream genes. To explore the epigenetic mechanism by which sodium oxamate alleviates neuropathic pain, we used Cut&Tag technology to compare H3K18la enrichment differences in spinal cord tissue between the Oxamate group and the CCI group to identify epigenetic alterations associated with the therapeutic effect. Among these, special attention was paid to differentially enriched peaks in promoter regions, because the promoter region is

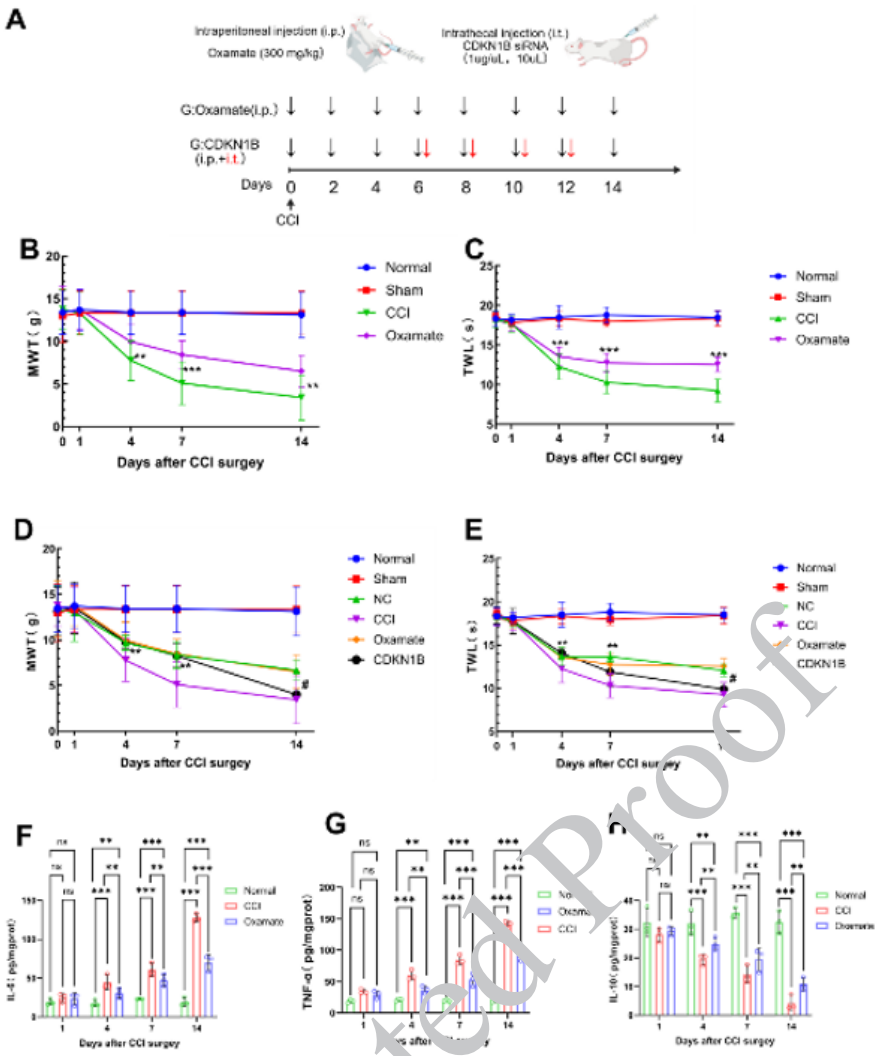

Figure 2. Behavioral analysis and changes in rat inflammatory mediator expression
(A) Schematic diagram of the experimental protocol and drug administration schedule.
(B–C) Time course of thermal withdrawal latency (B) and mechanical withdrawal threshold (C) in CCI rats after sodium oxamate treatment, showing improvement in pain-related behaviors.
(D–E) Changes in thermal withdrawal latency (D) and mechanical withdrawal threshold (E) following CDKN1B knockdown. *P<0.05, CDKN1B group vs CCI group; #P<0.05, CDKN1B group vs Oxamate group.
(F–H) Time-course changes and intergroup differences in the levels of the pro-inflammatory cytokines IL-6 (F) and TNF-α (G), and the anti-inflammatory cytokine IL-10 (H) in the spinal cord tissue of each group.
Data are expressed as mean±SD (n=3 rats per group for biochemical assays; n=6 for behavioral tests). *P<0.05, **P<0.01, ***P<0.001; ns, not significant. Statistical analyses were performed using two-way ANOVA followed by Tukey's *post hoc* test.
CCI: Chronic constriction injury; CDKN1B: Cyclin-dependent kinase inhibitor 1B; IL-6: Interleukin-6; IL-10: Interleukin-10; TNF-α: Tumor necrosis factor-α

key to gene transcriptional regulation, and the transcriptional activity of genes located within it is often more susceptible to regulation by changes in histone lactylation levels. Compared with the CCI group, 693 peaks with up-regulated H3K18la enrichment signals and 1131 peaks with down-regulated signals were identified in the Oxamate group. Among the up-regulated peaks, those located in promoter regions (within 3 kb upstream of the transcription start site) accounted for 9.81% (68 peaks). Based on literature reports and functional enrichment analysis, cyclin-dependent kinase inhibitor 1B (CDKN1B) was listed as a potential candidate target gene. This gene encodes the p27 protein, which is involved in biological processes such as cell cycle regulation, neuronal development, and autophagy. To further verify the expression changes of CDKN1B, qPCR was performed. The results showed (Figure 3 F-G): compared with the Normal group, the mRNA level of CDKN1B in the spinal cord tissue of rats in the CCI group was significantly decreased from postoperative day 4 and persisted until day 14; compared with the CCI group, the expression of CDKN1B in the Oxamate group was significantly up-regulated from postoperative day 4 onward; and compared with the Normal group, the CDKN1B level in the Oxamate group was also significantly elevated on postoperative days 7 and 14.

Intrathecal injection of CDKN1B siRNA reverses the analgesic effect of oxamate in CCI rats

To investigate the role of CDKN1B in pain, we performed intrathecal injection of CDKN1B siRNA in CCI rats that had received intraperitoneal sodium oxamate, with the primary aim of suppressing CDKN1B/p27 expression. The mRNA expression level of CDKN1B in the Oxamate group exhibited a statistically significant difference starting from day 7 after intraperitoneal oxamate injection; therefore, intrathecal injections were mainly performed on postoperative days 6,

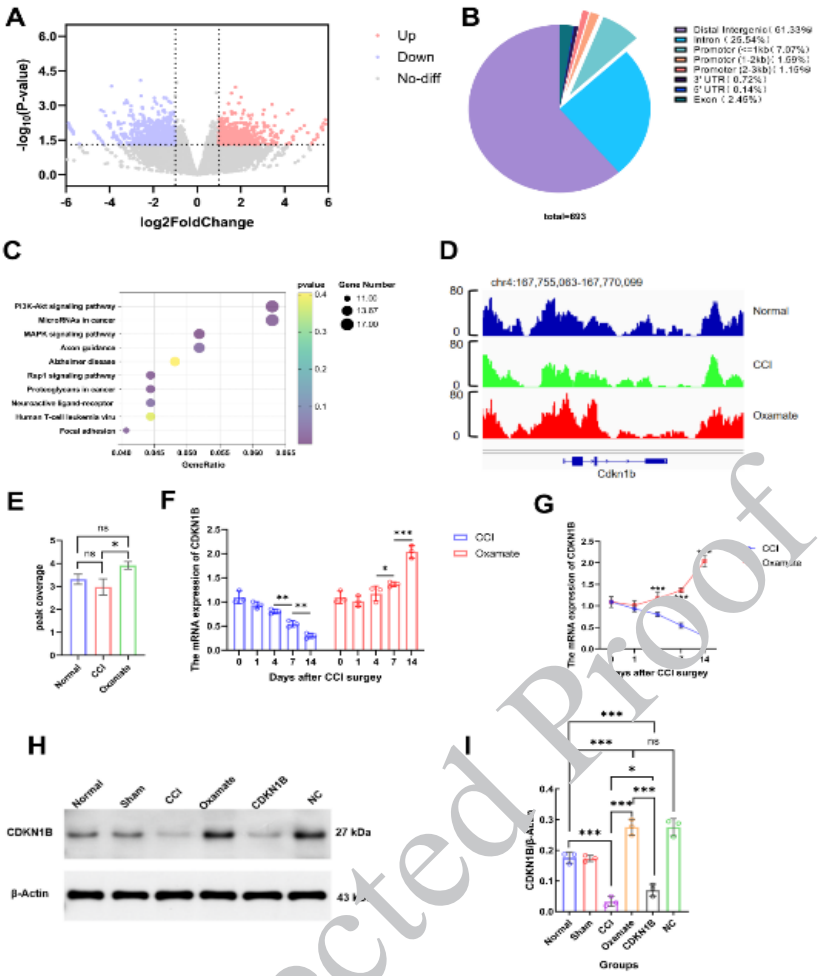

Figure 3. H3K18la promotes CDKN1B transcription in the rat Oxamate group
(A) Volcano plot of differential H3K18la enrichment peaks between the Oxamate and CCI groups. Red dots indicate significantly up-regulated peaks, and blue dots indicate significantly down-regulated peaks.
(B) Genomic distribution annotation of H3K18la-enriched peaks that were up-regulated in the Oxamate group relative to the CCI group.
(C) KEGG pathways enriched among the up-regulated peaks in the Oxamate vs CCI comparison.
(D) IGV genome browser views showing H3K18la read coverage at the CDKN1B gene locus across groups.
(E) Quantitative analysis of H3K18la enrichment at the CDKN1B promoter region (±500 bp around the transcription start site), showing a significantly higher enrichment score in the Oxamate group than in the CCI group.
(F-G) Time-course changes in CDKN1B mRNA relative expression levels in the spinal cord of each group, measured by real-time quantitative PCR.
(H) Representative western blot bands of CDKN1B protein in the spinal cord tissue of each group on postoperative day 14.
(I) Quantitative analysis of CDKN1B protein relative expression levels, with β-actin as the loading control.
Data are expressed as mean±SD (n=3 rats per group). *P<0.05, **P<0.01, ***P<0.001; ns, not significant. Comparisons were performed using one-way ANOVA followed by Tukey's *post hoc* test.
CCI: Chronic constriction injury; CDKN1B: Cyclin-dependent kinase inhibitor 1B; H3K18la: Histone H3 lysine 18 lactylation; IGV: Integrative genomics viewer; KEGG: Kyoto encyclopedia of genes and genomes

8, 10, and 12. To verify whether CDKN1B/p27 expression in the spinal cord tissue of Oxamate rats was reduced as expected after intrathecal CDKN1B siRNA injection, western blot analysis was conducted on spinal cord tissues collected on postoperative day 14. The results demonstrated that sciatic nerve ligation led to a significant decrease in CDKN1B/p27 protein expression in the spinal cord tissue compared with the normal control group; after inhibiting glycolysis and histone lactylation, CDKN1B/p27 expression was significantly increased on day 14; and subsequent intrathecal injection of CDKN1B siRNA significantly down-regulated CDKN1B/p27 expression in the spinal cord tissue, as shown in Figure 3 H–I. Subsequently, pain behavioral tests were performed on postoperative days 1, 4, 7, and 14. The detailed data are presented in Table 3. It was observed that Oxamate group rats receiving intrathecal CDKN1B siRNA from postoperative day 6 onward exhibited a resurgence of pain sensitivity on postoperative day 14, manifested as shortened thermal withdrawal latency and decreased mechanical withdrawal threshold. Their behavioral trend was closer to that of the CCI model group rather than the Oxamate group.

Intrathecal injection of CDKN1B siRNA attenuates autophagic activity in Oxamate group rats

To investigate whether CDKN1B/p27 participates in pain modulation through autophagy in CCI rats, we used Beclin-1 protein expression and the LC3-II/LC3-I ratio as indirect markers of autophagic activity—concomitant increases in both indicate enhanced autophagy, whereas concurrent decreases suggest suppression. These markers were assessed by western blot. On postoperative day 14, compared with the Normal and Sham groups, the expression of Beclin-1 and the LC3-II/LC3-I ratio in the spinal cord

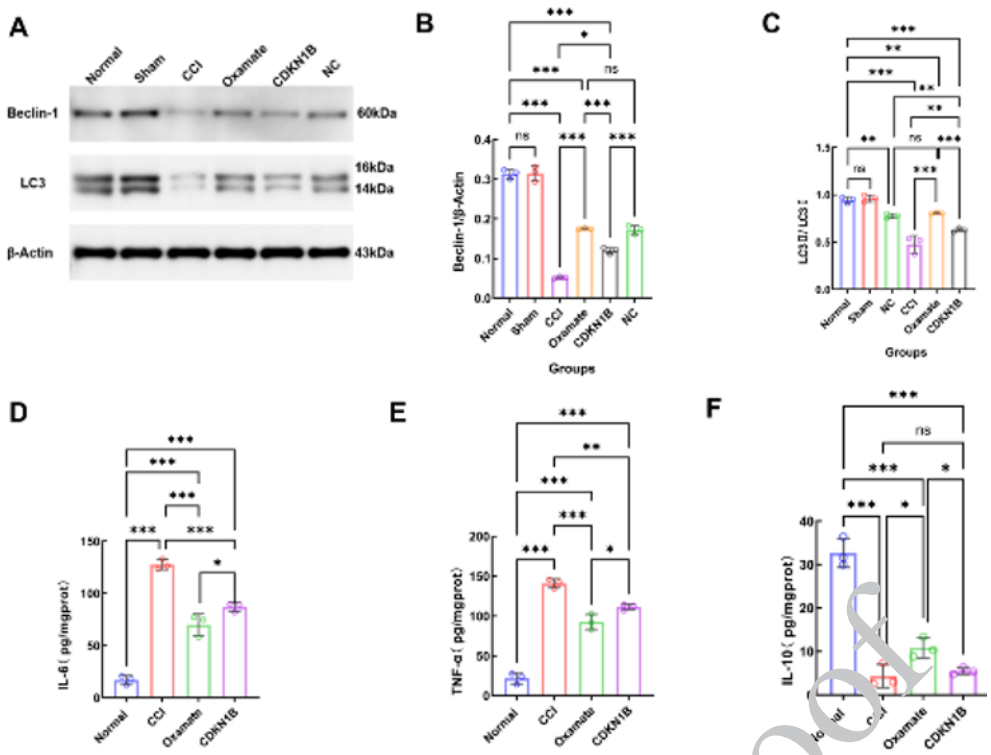

Figure 4. Expression levels of autophagy markers and inflammatory factors in the spinal cord tissue of each rat group on postoperative day 14
(A) Representative western blot bands of the autophagy-related proteins Beclin-1 and LC3-II/LC3-I.
(B) Quantitative analysis of Beclin-1 relative protein expression, with β-actin as the loading control.
(C) Quantitative analysis of the LC3-II/LC3-I ratio.
(D–F) Levels of the pro-inflammatory cytokines IL-6 (D) and TNF-α (E), and the anti-inflammatory cytokine IL-10 (F) in the spinal cord tissue of each group.
Data are expressed as mean±SD (n= 3 rats per group). *P<0.05, **P<0.01, ***P<0.001; ns, not significant. Statistical comparisons among groups were performed using one-way ANOVA followed by Tukey's *post hoc* test.
IL-6: Interleukin-6; IL-10: Interleukin-10; LC3: Microtubule-associated protein 1 light chain 3; TNF-α: Tumor necrosis factor-α.

tissue of CCI rats were significantly decreased. After sodium oxamate intervention, the autophagy indicators in the Oxamate group were significantly higher than those in the CCI group. Following further knockdown of CDKN1B expression by intrathecal injection of CDKN1B siRNA, the autophagy indicators in the CDKN1B group were significantly decreased compared with the Oxamate group. Still, they remained higher than those in the CCI group (Figure 4A-C). These results indicate that sciatic nerve ligation can inhibit autophagic activity in the spinal cord tissue; sodium oxamate enhances autophagic activity by up-regulating CDKN1B/p27 expression, and down-regulation of CDKN1B can partially reverse this effect.

Intrathecal injection of CDKN1B siRNA exacerbates the inflammatory response in Oxamate group rats

To explore the effect of down-regulating CDKN1B expression on the inflammatory response in the spinal cord tissue of rats, the expression levels of inflammatory cytokines in the spinal cord tissue of each group were measured by ELISA on postoperative day 14. The results showed (Figure 4D–F): compared with the Normal group, the levels of the pro-inflammatory cytokines IL-6 and TNF-α in the spinal cord tissue of the CDKN1B group were significantly increased, and the anti-inflammatory cytokine IL-10 was significantly decreased; compared with the CCI group, the levels of IL-6 and TNF-α in the CDKN1B group were significantly decreased, while IL-10 showed no statistically significant difference; compared with the Oxamate group, the levels of IL-6 and TNF-α in the CDKN1B group were significantly increased, and the IL-10 level was significantly decreased. In summary, intrathecal injection of CDKN1B siRNA reversed the anti-inflammatory effect of sodium oxamate, aggravated the inflammatory response, and the inflammatory level was negatively correlated with autophagic activity.

Discussion

Existing studies have confirmed that histone PTMs are involved in the development and maintenance of neuropathic pain, but current evidence has mainly focused on modifications such as acetylation and methylation. For example, in rat pain models induced by spinal nerve ligation (SNL) and complete Freund's adjuvant (CFA), acetylated histones H3 and H4 were localized in the nuclei of dorsal root ganglion neurons and glial cells, providing morphological evidence for histone modifications in pain pathways. Further studies have found that histone acetyltransferase or histone deacetylase inhibitors can alleviate hyperalgesia in animal models of chronic pain (22). In mouse models of neuropathic pain induced by CCI and spared nerve injury (SNI), the histone demethylase JMJD2A was shown to promote the expression of brain-derived neurotrophic factor (Bdnf), thereby facilitating neuropathic pain (23). In contrast, histone lactylation, a newly discovered form of PTM, remains in the early stages of research in the field of pain.

H3K18 lactylation (H3K18la) refers to the lactylation co-post-translational modification occurring at lysine 18

of the histone H3 subunit, mediated by lactyl-CoA as a donor, and represents a novel type of histone modification. Using the CCI rat model, this study investigated the role and mechanism of H3K18la in neuropathic pain. The results showed that from day 4 after sciatic nerve ligation, L-lactate content and H3K18la levels in the spinal cord increased simultaneously, accompanied by elevated pro-inflammatory cytokines IL-6 and TNF-α, and decreased anti-inflammatory IL-10, suggesting that local inflammatory imbalance contributes to the enhanced pain sensitivity. Following intraperitoneal injection of the glycolysis inhibitor sodium oxamate, both L-lactate levels and H3K18la expression were effectively reduced, along with improved pain behaviors and partial recovery of the inflammatory cytokine profile—specifically, declines in IL-6 and TNF-α together with an increase in IL-10. Collectively, these preliminary findings suggest that sodium oxamate may alleviate neuropathic pain at least in part by down-regulating H3K18la levels and rectifying local inflammatory imbalance.

To explore the epigenetic mechanism by which sodium oxamate alleviates neuropathic pain, we used CUT&Tag technology to compare the differences in H3K18la enrichment in the spinal cord tissue between the Oxamate group and the CCI group, and through differential analysis combined with literature screening, we identified CDKN1B as a potential downstream target gene regulated by H3K18la. Notably, while sodium oxamate reduced the global level of H3K18la in the spinal cord, it specifically enhanced H3K18la enrichment at the CDKN1B promoter region. This seemingly contradictory finding suggests that sodium oxamate does not simply suppress lactylation globally, but rather reshapes the genomic distribution of H3K18la, achieving a refined regulation of "withdrawal from non-critical sites and concentration on key targets." Similar phenomena have been reported in epigenetic studies of metabolic interventions; for instance, metformin regulates the activity of various histone acetylation-related enzymes through AMPK, enabling selective regulation of different gene promoter regions (24-25). This mechanism implies that under metabolic stress, the organism preferentially activates certain protective genes (such as CDKN1B) to promote autophagy, reduce inflammation, and relieve pain.

It should be noted that we employed CUT&Tag as the core technique for detecting H3K18la enrichment. This method offers relatively low background noise and a high signal-to-noise ratio, allowing reasonably precise mapping of histone modification distribution across the genome. In our study, CUT&Tag revealed significantly increased H3K18la enrichment at the CDKN1B promoter region in the Oxamate group compared with the CCI group; concurrently, both qPCR and western blot confirmed consistent up-regulation of CDKN1B at the mRNA and protein levels. Furthermore, the CDKN1B siRNA knockdown experiments functionally validated the necessity of this gene in autophagy regulation, inflammatory responses, and pain behaviors—knockdown partially reversed the effects of sodium oxamate. Taken together, these findings provide multilayered evidence—from modification enrichment, to expression changes, to functional phenotypes—supporting the proposed regulation of CDKN1B transcription by H3K18la. Admittedly, more direct approaches such as ChIP-qPCR or site-directed mutagenesis would be required to strengthen further the causal evidence, which is precisely one of the limitations acknowledged in our study.

In the tests conducted on postoperative day 14, compared with the Normal group, the CCI group showed decreased expression of CDKN1B mRNA and p27 protein, as well as reduced autophagic proteins Beclin-1 and the LC3-II/LC3-I ratio; following sodium oxamate intervention, all these indicators were reversed. After intrathecal injection of CDKN1B siRNA, autophagic activity was again suppressed, the pain threshold decreased, and the cytokine profile shifted toward a pro-inflammatory direction. Taken together, these results allowed us to propose and validate a signaling axis: glycolysis inhibition → reduced lactate and histone H3K18la levels → H3K18la specifically drives CDKN1B up-regulation → enhanced autophagy → inflammation alleviation → pain relief.

When analyzing the data, we also noticed a noteworthy phenomenon: the enrichment of H3K18la and the expression of CDKN1B were not completely parallel. Specifically, between the CCI group and the Normal group, there was no significant difference in H3K18la enrichment at the CDKN1B promoter ($P > 0.05$), yet the mRNA and protein levels were significantly down-regulated ($P<0.05$). In contrast, between the Oxamate group and the CCI group, both showed consistent and significant up-regulation. We propose several possible explanations for this. First, the regulation of transcription by histone modifications may exhibit a threshold effect (26) — only when the enrichment of a modification exceeds a certain critical level can it effectively trigger gene expression; minor changes below the threshold, even if not statistically significant, may still cause alterations in functional output. That is, the slight decrease of H3K18la in the CCI group may have already crossed the critical point for transcriptional permission at the CDKN1B promoter, leading to a shutdown of its transcription. Second, CDKN1B transcription is coordinately regulated by multiple epigenetic modifications and transcription factors, and other inhibitory mechanisms in the CCI model may act synergistically with the slight decrease in H3K18la, jointly resulting in the significant down-regulation of expression (27). Third, CUT&Tag detects the absolute abundance of modifications, whereas qPCR/western blot detects the functional transcriptional output; the two have different dynamic ranges, and the latter is more sensitive to minor changes. However, it should be emphasized that the core finding of this study — "sodium oxamate significantly increases H3K18la enrichment at the CDKN1B promoter and up-regulates its expression" — is robust and consistent in the Oxamate vs CCI comparison, and therefore does not affect the conclusion that CDKN1B is a key downstream effector molecule of sodium oxamate. Instead, this phenomenon suggests that the gene has a specific response to metabolic intervention, providing a basis for its potential as a therapeutic target.

The study by Wang et al. also provides strong supporting evidence. They found that in the injured dorsal root ganglia (DRGs) of CCI mice, H3K18la levels were up-regulated, which in turn activated the transcription of insulin-like growth factor 2 mRNA-binding protein 2 (Igf2bp2) and up-regulated CCT2 protein expression, ultimately inducing pain behaviors. Inhibition of H3K18la alleviated pain (28). This pattern of action shares many similarities with the mechanism we observed, in which H3K18la promotes CDKN1B expression, enhances autophagy, and participates in pain regulation, further supporting the notion that H3K18la serves as a core epigenetic regulatory node that

can engage different downstream target genes to contribute to pain development.

The protein product encoded by CDKN1B, p27, is a typical intrinsically disordered protein with a highly flexible conformation, and its functional activity is jointly regulated by expression levels, subcellular localization, and various PTMs. Beyond its classical role as a negative regulator of the cell cycle through inhibition of cyclin-dependent kinase (CDK) activity, the non-canonical functions of p27 have garnered increasing attention. It can interact with multiple molecules as a "scaffold" and participate in processes such as autophagy regulation, gene transcription, and signal transduction. Studies have shown that under various stress conditions such as prolonged amino acid starvation, glucose deprivation, or cellular senescence, p27 can promote autophagy through multiple mechanisms, exerting a cytoprotective effect.

The development of neuropathic pain involves the activation of microglia and astrocytes, as well as the infiltration of immune cells into the ganglia. These processes release pro-inflammatory cytokines and enhance neuronal excitability, thereby inducing and maintaining the pain state. Autophagy may exert an inhibitory regulatory role in both the induction and maintenance phases of pain through the modulation of inflammatory cytokines (29-30). In a CFA-induced inflammatory pain model, exosomes derived from human umbilical cord mesenchymal stem cells (huc-MSCs) reduced neuroinflammation by increasing the expression of LC3-II and Beclin1 and inhibiting the activation of the NLRP3 inflammasome in the spinal dorsal horn; the use of 3-MA (an autophagy inhibitor) could attenuate this protective effect (31). In the CCI model, diosgenin extracted from yam alleviated pain by enhancing autophagy and promoting microglial M2 polarization, and the autophagy inhibitor chloroquine could reverse this effect (32). In our study, autophagic activity in the spinal cord tissue showed a clear negative correlation with inflammatory levels. In the CCI group, the autophagy markers Beclin-1 and the LC3-II/LC3-I ratio were significantly decreased, accompanied by increased pro-inflammatory cytokines IL-6 and TNF-α and decreased anti-inflammatory cytokine IL-10; after sodium oxamate treatment, autophagic activity rebounded, and the inflammatory response was reversed; and following CDKN1B knockdown, autophagic activity declined again, and the inflammatory response was re-aggravated. This series of dynamic changes suggests that autophagy acts as an "inflammatory brake" in neuropathic pain: enhanced autophagy suppresses pro-inflammatory responses, while impaired autophagy lifts the inflammatory constraint. Therefore, sodium oxamate enhancing spinal autophagy through up-regulation of CDKN1B/p27, thereby inhibiting neuroinflammation, represents an important mechanism for its pain-relieving effect.

The novelty of this study lies mainly in three aspects. First, this study introduced histone lactylation modification into the research of neuropathic pain. It provided initial observations on the specific changes of H3K18la, offering a new perspective and exploratory experimental basis for the application of epigenetics in the pain field. Second, we organically linked glycolysis metabolism, histone lactylation, and autophagy regulation, attempting to construct a complete "metabolism–epigenetics–function" mechanistic chain. Third, we used CUT&Tag technology to screen differentially enriched regions across the genome, combined with functional validation, which improved the precision and reliability of target gene screening to a certain extent.

Several limitations of this study should be acknowledged when interpreting the findings. First, all experiments were conducted solely in the rat CCI model, without validation in other pain models or human samples; accordingly, the translational value of our results remains preliminary. Second, autophagic activity was assessed mainly via protein markers including Beclin-1 and the LC3-II/LC3-I ratio, without electron microscopic morphological evidence or autophagic flux blockade experiments, which restricts a full interpretation of autophagic processes. Third, although CUT&Tag analysis has revealed genome-wide changes in H3K18la enrichment, more direct experimental approaches are needed to strengthen the evidence for its targeted regulatory effects.

To address these limitations, future studies may consider the following directions: (1) validation in additional neuropathic pain models (e.g., SNI, SNL) and human samples to enhance the generalisability and translational relevance of the conclusions; (2) incorporation of transmission electron microscopy or autophagic flux blockers such as chloroquine to more comprehensively evaluate autophagic degradation integrity; and (3) use of ChIP-qPCR or CRISPR-mediated site-directed mutagenesis to more rigorously verify the direct causal relationship between H3K18la and CDKN1B transcription. In addition, extending the postoperative observation period would help assess the long-term stability and potential side effects of this pathway. Overall, this study, starting from metabolism, taking epigenetic modifications as a perspective, and focusing on autophagy and inflammation, preliminarily explored the potential regulatory role of histone lactylation in neuropathic pain, providing a new entry point for pain biology research.

Conclusion

Sciatic nerve ligation can lead to elevated L-lactate content and H3K18la expression levels in the spinal cord tissue of rats, accompanied by down-regulation of CDKN1B expression and suppressed autophagic activity, along with an imbalance of inflammatory mediators that ultimately induces pain behaviors.

Sodium oxamate, although it reduces global lactate levels and H3K18la expression, can specifically enhance H3K18la enrichment at the CDKN1B promoter region, thereby up-regulating CDKN1B expression and activating autophagy to exert an analgesic effect.

This study indicates that the protective role of autophagy in pain modulation is primarily achieved through the negative regulation of inflammatory mediators.

Acknowledgment

We sincerely thank all members of our research group for their support and collaboration during this study.

Funding

This study was supported by Guangdong Basic and Applied Basic Research Fund - Regional Joint Fund (No. 2023A1515140052; No.2023A1515140048), and the Hospital Level Project of Foshan Second People's Hospital (No. A2022A01).

Institutional Review Board Statement

The study protocol received approval from the Animal Ethics Committee of Guangdong Medical Laboratory Animal Center (Ethics Approval Number: C202309-38).

Data Availability Statement

If needed, data can be provided by WX.

Authors' Contribution

All authors contributed to the design and review of the manuscript. XJ O was responsible for designing and carrying out the experiments and writing the paper. FT Z, L L, and MY Z performed the experiments, collected data, and conducted statistical analyses. WC Z and XJ W supervised, directed, and managed the study. XJ W also oversaw the overall research design and provided guidance, in addition to performing the final review of the manuscript.

Conflicts of Interest

The authors declare no potential conflicts of interest regarding the research, authorship, or publication of this article.

Declaratin

During the preparation of this manuscript, the authors used DeepL to assist with language translation and polishing. The authors take full responsibility for the content of this publication. All data analysis, interpretation of results, figure preparation, and writing of the core scientific content were performed by the authors without AI assistance.

References

1. Cohen S P, Vase L, Hooten W M. Chronic pain: An upda... on burden, best practices, and new advances. Lancet. 2021; 397: 2082-2097.
2. Hooten W M. Chronic Pain and Mental Health Disorders: Shared Neural Mechanisms, Epidemiology, and Tr...atment. Mayo Clin Proc 2016;91:955-70.
3. van Hecke O, Austin SK, Khan RA, Smith BH, Torrance N. Neuropathic pain in the general population: A systematic review of epidemiological studies. Pain 2014;155:654-662.
4. Yan YY, Li CY, Zhou L, A... LY, Fa... WJ, Li YM. Research progress of mechanisms and drug therapy for neuropathic pain. Life Sci 2017; 190: 68-77.
5. Glick D, Barth S, Macleod K... Autophagy: Cellular and molecular mechanisms. J Pathol 2010; 221: 3-12.
6. Liao MF, Lu KT, Hsu JL, Lee CH, Cheng MY, Ro LS. The role of autophagy and apoptosis in neuropathic pain formation. Int J Mol Sci 2022; 23: 2685.
7. Torres-Perez JV, Irfan J, Febrianto MR, Di Giovanni S, Nagy I. Histone post-translational modifications as potential therapeutic targets for pain management. Trends Pharmacol Sci 2021; 42: 897-911.
8. Ghosh K, Pan H L. Epigenetic mechanisms of neural plasticity in chronic neuropathic pain. ACS Chem Neurosci 2022; 13: 432-441.
9. Borgonetti V, Meacci E, Pierucci F, Romanelli MN, Galeotti N. Dual HDAC/BRD4 inhibitors relieves neuropathic pain by attenuating inflammatory response in microglia after spared nerve injury. Neurotherapeutics 2022; 19: 1634-1648.
10. Zhang D, Tang Z, Huang H, Zhou G, Cui C, Weng Y, *et al.* Metabolic regulation of gene expression by histone lactylation. Nature 2019; 574: 575-580.
11. Xu K, Zhang K, Wang Y, Gu Y. Comprehensive review of histone lactylation: Structure, function, and therapeutic targets. Biochem Pharmacol 2024; 225: 116331.
12. Lan Q, Ouyang A, Chen Y, Li Y, Zhong B, Deng S. Pain, lactate, and anesthetics: Intertwined regulators of tumor metabolism and immunity. Front Oncol 2025; 15: 1534300.
13. Wang Y, Peng Y, Zhang C, Zhou X. Astrocyte-neuron lactate transport in the ACC contributes to the occurrence of long-lasting inflammatory pain in male mice. Neurosci Lett 2021; 764: 136205.
14. Bennett GJ, Xie YK. A peripheral mononeuropathy in rat that produces disorders of pain sensation like those seen in man. Pain 1988;33:87-107.
15. Shan L, Xu K, Ji L, Zeng Q, Liu Y, Wu Y, *et al.* Injured sensory neurons-derived galectin-3 contributes to neuropathic pain via programming microglia in the spinal dorsal horn. Brain Behav Immun 2024, 117: 80-99.
16. Tan PH, Gao YJ, Berta T, Xu ZZ, Ji RR. Short small-interfering RNAs produce interferon-α-mediated analgesia. Br J Anaesth 2012;108: 662-669.
17. Ledent C, Valverde O, Cossu G, Petitet F, Aubert JF, Beslot F, *et al.* Unresponsiveness to cannabinoids and reduced addictive effects of opiates in CB1 receptor knockout mice. Science 1999;283:401-404.
18. Hanus L, Breuer A, Tchilibon S, Shiloah S, Goldenberg D, Horowitz M, *et al.* HU-308: A specific agonist for CB(2), a peripheral cannabinoid receptor. Proc Natl Acad Sci U S A 1999;96:14228-14233.
19. Zimmer A, Zimmer AM, ...hmann AG, Herkenham M, Bonner TI. Increased mor...l, hyp...activity, and hypoalgesia in cannabinoid CB1 receptor knock...ut mice. Proc Natl Acad Sci U S 1999; 96: 5780-5785.
20. Hu X, Huang J, Li Z, ...i J, Ouyang F, Chen Z, *et al.* Lactate promotes microglial ...ar formation and facilitates locomotor function rec...very by enhancing histone H4 lysine 12 lactylation after spi...l cord injury. J Neuroinflammation 2024;21: 193.
21. Díaz-G...cía C M. Glycogen from spinal astrocytes dials up the p...n. Nat Me...b 2024;6: 384-386.
22. ...iang L, Tao Y X. Expression of acetyl-histone H3 and acetyl-h...stone H4 in dorsal root ganglion and spinal dorsal horn in rat ch...ic pain models. Life Sci 2018; 211: 182-188.
23. Zhou J, Wang F, Xu C, Zhou Z, Zhang W. The histone ...emethylase JMJD2A regulates the expression of BDNF and mediates neuropathic pain in mice. Exp Cell Res 2017;361: 155-162.
24. Vancura A, Vancurova I. Metformin induces protein acetylation in cancer cells. Oncotarget 2017;8: 39939.
25. Bridgeman SC, Ellison GC, Melton PE, Newsholme P, Mamotte CDS. Epigenetic effects of metformin: From molecular mechanisms to clinical implications. Diabetes Obes Metab 2018;20:1553-1562.
26. Policarpi C, Munafò M, Tsagkris S, Carlini V, Hackett JA. Systematic epigenome editing captures the context-dependent instructive function of chromatin modifications. Nat Genet 2024;56: 1168-1180.
27. Vaissière T, Sawan C, Herceg Z. Epigenetic interplay between histone modifications and DNA methylation in gene silencing. Mutat Res 2008;659:40-48.
28. Wang QH, Xie S, Yang KH, Guo YX, Huang HY, Li SY, *et al.* Histone lactylation contributes to neuropathic pain by facilitating m6A reader protein IGF2BP2 expression in DRG sensory neurons. J Neurosci 2026;46:e0365252025.
29. Liao MF, Lu KT, Hsu JL, Lee CH, Cheng MY, Ro LS. The role of autophagy and apoptosis in neuropathic pain formation. Int J Mol Sci 2022;23: 2685.
30. Li L, Li T, Qu X, Sun G, Fu Q, Han G. Stress/cell death pathways, neuroinflammation, and neuropathic pain. Immunol Rev 2024; 321:33-51.
31. Hua T, Yang M, Song H, Kong E, Deng M, Li Y, *et al.* Huc-MSCs-derived exosomes attenuate inflammatory pain by regulating microglia pyroptosis and autophagy via the miR-146a-5p/TRAF6 axis. J Nanobiotechnology 2022;20:324.
32. Man S, Zhou Y, Zhang X, Tang X, Xie L, Ma L, *et al.* Diosgenin alleviates neuropathic pain based on the enhancement of autophagy and promotion of M2 polarization. Int Immunopharmacol 2025;159:114936.